J Mol Med (2009) 87:1191–1205
DOI 10.1007/s00109-009-0530-8

ORIGINAL ARTICLE

Induction of *Foxp3* demethylation increases regulatory $CD4^+CD25^+$ T cells and prevents the occurrence of diabetes in mice

Qanhui Zheng · Yamei Xu · Yanlong Liu · Baojun Zhang · Xiaokun Li · Feng Guo · Yong Zhao

Received: 10 December 2008 / Revised: 2 August 2009 / Accepted: 26 August 2009 / Published online: 20 October 2009

Abstract $CD4^+CD25^+$ regulatory T cells (Treg), a subpopulation of $CD4^+$ T cells, regulate immune responses. Foxp3 is a key transcription factor for the development and function of Treg cells. During T-cell activation in vitro, a DNA demethylation agent 5-Aza-2′-deoxycytydine (DAC) can induce Foxp3 expression in $CD4^+CD25^-$ $Foxp3^-$ cells via altering methylation status of a conserved element in the 5′-untranslated region of the *Foxp3* gene. However, the effects of this agent on the development of $Foxp3^+$ Treg cells in the thymus and in vivo are poorly understood. In the present study, a short-term treatment with a low dose of DAC significantly increased the ratios of thymic $CD4^+CD8^-$ $CD25^+$ cells or $CD4^+CD8^-$ $Foxp3^+$ cells to $CD4^+CD8^-$ cells, and the total numbers of thymic $CD4^+CD8^-Foxp3^+$ Treg cells or $CD4^+CD8^-CD25^+Foxp3^+$ Treg cells in the thymus in mice. DAC-treatment induced the Foxp3 expression and the significant demethylation of a CpG island in the first intron of the *Foxp3* gene in $CD4^+CD8^-CD25^+$ cells predominantly. Furthermore, $CD4^+CD8^-CD25^+$ thymocytes in DAC-treated mice exhibited enhanced immunosuppressive function than those in control mice. In addition, DAC treatment in vivo was effective in improving the clinical course of diabetes in cyclophosphamide (CY)-potentiated non-obese diabetic mice (CY-NOD). Thus, the in vivo treatment with DAC can significantly promote the development of natural thymic $CD4^+CD25^+Foxp3^+$ Treg cells through *Foxp3* demethylation, implicating a therapeutic application of DAC in patients suffering from autoimmune diseases.

Keywords Thymocytes · Regulatory T cells · Epigenetic · Development · Autoimmune disease

Abbreviations

Treg	Regulatory T cell
DP	Double positive
DN	Double negative
SP	Single positive
Foxp3	Forkhead box protein 3
CTLA-4	Cytotoxic T-lymphocyte-associated protein 4
GITR	Glucocorticoid-induced tumor necrosis factor receptor

Electronic supplementary material The online version of this article (doi:10.1007/s00109-009-0530-8) contains supplementary material, which is available to authorized users.

Q. Zheng · Y. Liu · B. Zhang · Y. Zhao (✉)
Transplantation Biology Research Division, State Key Laboratory of Biomembrane and Membrane Biotechnology, Institute of Zoology, Chinese Academy of Sciences, Beichen West Road 1-5, Chaoyang, Beijing, China 100101
e-mail: zhaoy@ioz.ac.cn

Q. Zheng · B. Zhang · Y. Zhao
China-U.S. Research Center for Life Sciences, Chinese Academy of Sciences, Beijing, China

Y. Xu
Department of Hematology, Dongzhimen Hospital, Beijing University of Traditional Chinese Medicine, Beijing 100700, China

Y. Liu · X. Li
Key Laboratory of Biotechnology Pharmaceutical Engineering of Zhejiang Province, School of Pharmaceutical Science, Wenzhou Medical College, Wenzhou, China

F. Guo (✉)
Central Lab, The First Affiliated Hospital of Soochow University, Shizi Road 188, Suzhou, China 215006
e-mail: guofeng27@suda.edu.cn

FCM	Flow cytometry
FITC	Fluorescein isothiocyanate
PE	Phycoerythrin
PI	Propidium iodide
LNs	Lymph nodes
PBMC	Peripheral blood mononuclear cells
MFI	Median fluorescence intensity
bp	Base pair
CY	Cyclophosphamide
NOD	Non-obese diabetes

Introduction

$CD4^+CD25^+$ regulatory T cells (Treg cells) are a subpopulation of $CD4^+$ T cells that are critical for maintaining self-tolerance and negatively regulating immune responses [1]. Development of $CD4^+CD25^+$ Treg cells mainly occurs in thymus, though some $CD4^+CD25^+$ Treg cells can be generated in the periphery in the context of suboptimal TCR stimulation [2–6]. The forkhead box transcription factor Foxp3 has been identified as a specific molecular marker for $CD4^+CD25^+$ Treg cells. Detailed studies showed that Foxp3 is essential and sufficient for the development and the function of $CD4^+CD25^+$ Treg cells in mice and humans [5, 7–11]. Generation of natural $Foxp3^+$ Treg cells occurs preferentially at CD4 single positive (SP) stage, and a significant proportion of developing T cells likely commit to $CD4^+CD25^+$ Treg cell lineage within the thymus [12–14]. On the other hand, it was proposed that the development of $Foxp3^+$ Treg cells is substantially delayed relative to non-regulatory thymocytes during ontogeny [12, 15]. However, the mechanism controlling the Foxp3 expression in the developing $CD4^+CD25^+$ Treg cells in thymus is not known so far.

Epigenetic control including DNA methylation and histone modifications is a well-established means of gene regulation within the immune system [16, 17]. Recently, several studies have demonstrated that the Foxp3 expression during T cell activation is strictly controlled by an evolutionarily conserved element overlapping a CpG island, which is located in the *Foxp3* first intron. Methylation of this CpG island inversely correlates with Foxp3 expression during the induction of peripheral $CD4^+CD25^+$ Treg cells [17, 18]. The in vitro treatment of $CD4^+CD25^-$ cells with the demethylating agent 5-Azacytidine or 5-Aza-2′-deoxycytidine (DAC) results in demethylation at the *Foxp3* locus and the elevated Foxp3 expression [17, 19–22]. However, the in vivo effect of this agent on the expression of Foxp3 and $CD4^+CD25^+$ Treg cells remains to be clarified. In the present study, we found that the treatment with a low dose of DAC significantly enhanced the ratios of $CD25^+CD4SP$ cells or $Foxp3^+CD4SP$ cells to CD4 SP cells, and the total number of $Foxp3^+CD4$ SP cells with significant *Foxp3* gene demethylation in $CD25^+CD4SP$ cells. Moreover, DAC treatment in vivo enhanced the Treg-mediated suppression of homeostatic proliferation and decreased the occurrence of diabetes of CY-potentiated NOD mice.

Materials and methods

Mice C57BL/6 mice (6-week-old' male) and NOD/LtJ (5-week-old' female) mice were purchased from Beijing Laboratory Animal Research Center (Beijing, China). All mice were maintained in specific pathogen-free facility and were housed in microisolator cages containing sterilized feed, autoclaved bedding, and water. To synchronize and accelerate the development of diabetes, NOD mice were given a single intraperitoneal injection (250 mg/kg body weight) of cyclophosphamide (CY) at 8 weeks old. Non-fasting blood glucose was measured every week with a glucose meter (Freestyle) and mice were considered diabetic when the blood glucose level was over 11.1 mM [23]. All experimental manipulations were undertaken in accordance with the institutional guideline.

Reagents 5-Aza-2′-deoxycytidine (DAC) was obtained from Sigma. A 2-mg/ml solution of DAC was prepared in dimethyl sulfoxide (DMSO, Sigma) and stored as small aliquots at −80°C. For C57BL/6 mice, DAC was administered intraperitoneally at a dose of 0.15 mg/kg/day for 5 days, NOD mice were administered intraperitoneally at a dose of 0.1 mg/kg/day for 5 weeks. Mitomycin C ($C_{15}H_{18}N_4O_5$) was obtained from Kyowa Hakko (Tokyo, Japan). The culture medium was RPMI 1640 (Hyclone, Logan, UT) supplemented with 10% heat-inactivated fetal calf serum, 100 U/ml penicillin, 100 μg/ml streptomycin, 2 mM L-glutamine, 10 mM HEPES, 1 mM sodium pyruvate, and 50 μM 2-mecaptoethanol (2-ME; Sigma, St. Louis, MO). [^{3}H] thymidine was purchased from China Institute of Atomic Energy (Beijing, China)

Monoclonal antibodies The following monoclonal antibodies (mAbs) were purchased from either BD Biosciences PharMingen (San Diego, CA) and eBioscience (San Diego, CA). Fluorescein isothiocyanate (FITC)-labeled anti-mouse CD4 mAbs (RM4-5; rat IgG2a), Phycoerythrin-CY5 (PE-CY5) labeled anti-mouse CD4mAb (H129.19; rat IgG2a), FITC-labeled anti-mouse CD8a mAb (53-6.7; rat IgG2a), PE-labeled anti-mouse CD8a mAb (53-6.7; rat IgG2a), FITC-labeled anti-mouse CD25 mAb (7D4; rat IgM), PE-labeled anti-mouse CD25 mAb (PC61.5; rat IgG1), PE-labeled anti-mouse CD45RB mAb (16A; rat IgG2a), PE-labeled anti-mouse CD62L mAb (SK11; rIgG2a), PE-labeled anti-mouse GITR mAb (DTA-1; rat

IgG2b), PE-labeled anti-mouse CD152 mAb (BNI3; mIgG2a). In addition, PE-labeled anti-mouse Foxp3 mAb (FJK-16s; rat IgG2a) and the staining kit were obtained from eBioscience (San Diego, CA). Rat anti-mouse FcR mAbs (2.4G2; IgG2b) were produced by 2.4G2 hybridoma (ATCC, Rockville, Maryland) in our laboratory.

Cell preparation Mouse peripheral blood mononuclear cells (PBMCs) were isolated by Ficoll gradient (Sigma, St. Louis, MO) described previously [24]. After DAC treatment for the indicated time, thymus, spleen, and lymph nodes (LNs including cervical, inguinal, and axillary LNs) were harvested. Single-cell suspensions were prepared by grinding the tissues with the plunger of a 5-ml disposable syringe and were then suspended in RPMI1640 medium. Splenocytes were treated with a hemolytic buffer (17 mM Tris–HCl and 140 mM NH_4Cl, pH 7.2) to remove red blood cells as described before [25].

Immunofluorescence staining and flow cytometry (FCM) Lymphocytes from thymus, spleen, LNs or PBMC were incubated with 2.4G2 to block FcRs and then incubated with an optimal concentration of fluorochrome-labeled mAbs for 30 min at 4°C in the dark. Cells were washed three times and resuspended by FCM buffer (PBS with 0.1% BSA and 0.1% NaN_3). At least 10,000 cells were assayed using a FACSCalibur flow cytometry (Becton Dickinson, CA). Data were analyzed with CellQuest software (Becton Dickinson, Mountain View, CA). In some experiments, nonviable cells were excluded using the vital nucleic acid stain propidium iodide (PI). The percentage of cells stained with a particular reagent or reagents was determined by subtracting the percentage of cells stained nonspecifically with the control mAb from staining in the same dot-plot region with the anti-mouse mAbs. For the intracellular staining, cells were incubated with PE-Cy5-labeled anti-CD4 and FITC-labeled anti-CD8 or

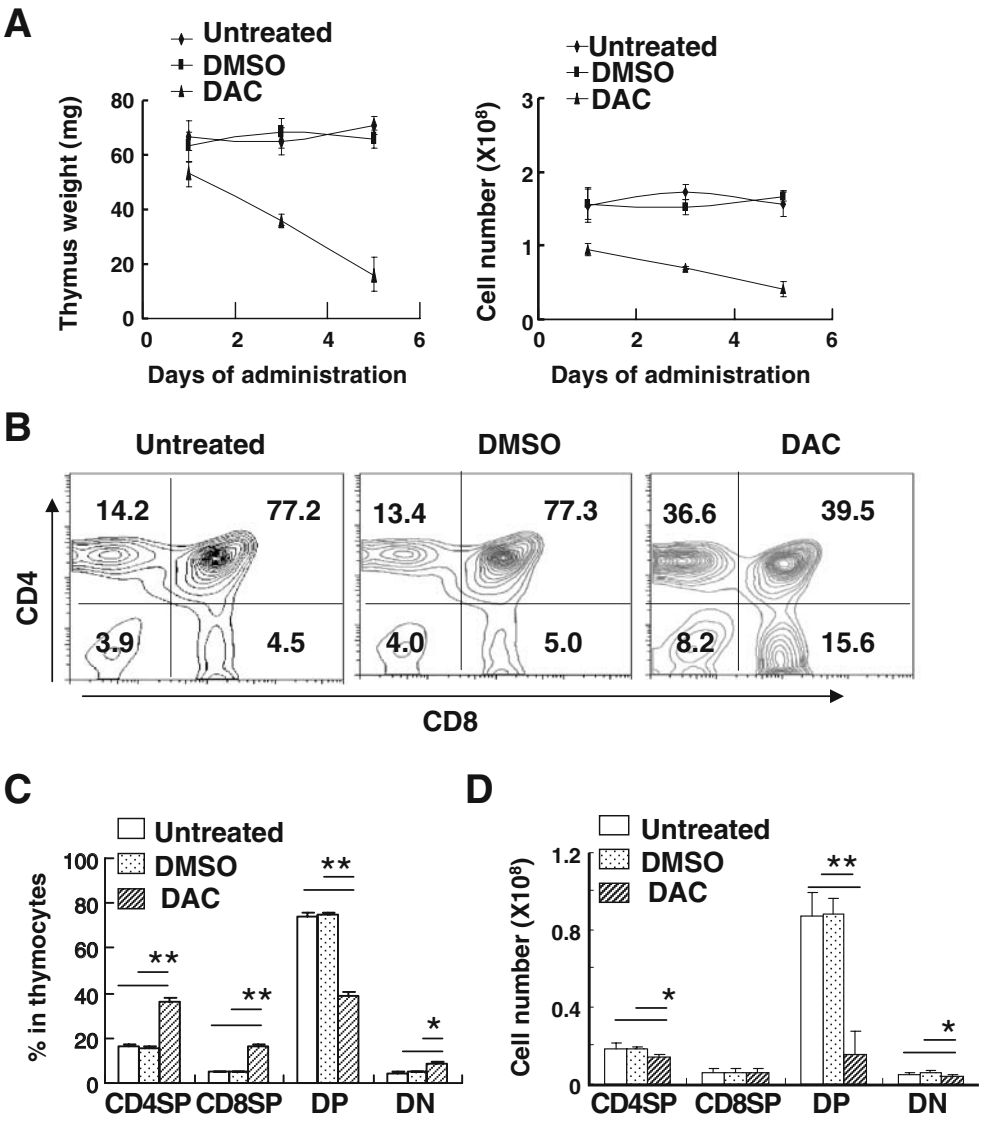

Fig. 1 Changes in cell number and composition of thymocytes in DAC-treated mice. **a** Decreased weight of thymus and thymocyte numbers in DAC-treated mice in the indicated time points. **b** Representative FACS samples demonstrating thymic subsets in control and DAC-treated mice. Thymocytes were stained with PE-Cy5-labeled anti-CD4 mAb and FITC-labeled anti-CD8 mAb, and analyzed by FCM. The percentage (**c**) and the total cell number (**d**) of DN, DP, CD4 SP, and CD8 SP subpopulations in DAC-treated mice for 5 days are summarized. *Asterisk*, $P<0.05$; *double asterisk*, $P<0.01$ compared with the control mice. Results were shown as mean ± SD ($N=5$), which is one representative of three independent experiments

anti-CD25 mAbs. After washing, these cells were then stained with PE-labeled anti-mouse Foxp3 mAb, or PE-labeled anti-mouse CD152 mAb according to the instruction offered by the manufacturer (eBiosciences, San Diego, CA).

Cell cycle and apoptosis analysis by FCM Thymocytes from DMSO- or DAC-administrated mice were fixed with 70% ethanol overnight. After being treated with 100 mg/ml of RNaseA (Sigma), Propidium iodide (PI 10 mg/ml; Sigma) was added to the cells for staining. The DNA contents were measured by FCM. For apoptosis analysis, thymocytes from the DMSO and DAC-administrated mice were harvested and stained with PI and Annexin V for 15 min at RT. Apoptosis was analyzed by fluorescence-activated cell sorting (FACS) using Coulter EPICS and ModFit software (Verity Software House, Topsham, MN).

RT-PCR DP and CD4SP thymocytes or $CD25^{+}CD4SP$ and $CD25^{-}CD4SP$ cells from DMSO and DAC-treated mice were sorted by FCM; RNA was extracted using

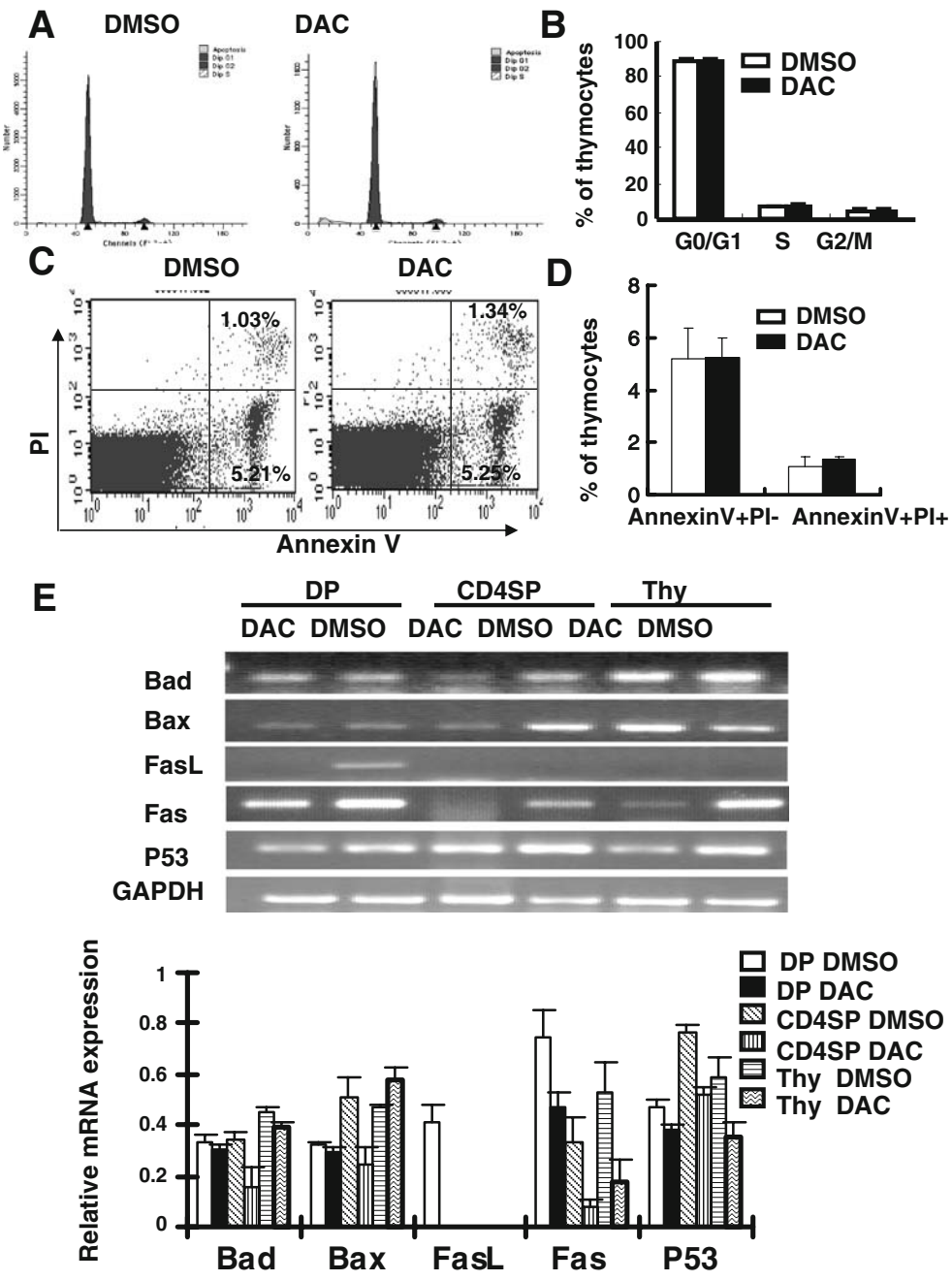

Fig. 2 No significant changes of cell cycle distribution and apoptosis of thymocytes in DAC-treated mice. **a** One representative cell cycle staining of thymocytes in DMSO and DAC-treated mice. **b** Cell cycle distribution of thymocytes in DMSO and DAC-treated mice was summarized. **c** One representative PI and Annexin V staining of thymocytes in DMSO and DAC-treated mice. **d** The percentage of Annexin $V^{+}PI^{-}$ and annexin$V^{+}PI^{+}$ thymocytes (apoptosis cells) in DMSO and DAC-treated mice was summarized. Results were shown as mean ± SD (N=5), which is one representative of three independent experiments. **e** RT-PCR analysis of Bad, Bax, FasL, Fas, and p53 mRNAs in total thymocytes, CD4SP and DP thymocytes in DMSO and DAC-treated mice. Expressions of Bad, Bax, FasL, Fas, and p53 mRNAs were semi-quantitatively analyzed by comparing the gray scale of GAPDH, which is one representative of two independent experiments

RNeasy Mini Kit (Qiagen) according to the manufacture's protocol. Reverse transcription reactions were performed using ThermoScriptTM RT-PCR System (Invitrogen) and using an oligo(dT)20 primer. PCR amplification to detect first strand cDNA for Bad, Bax , FasL, Fas, p53, Foxp3, TGFβ and GAPDH mRNA used the flowing primers: Bad, forward 5′-aggacttatcagccgaagca-3′, reverse 5′-gctcaaactctgggatctgg-3′; Bax, forward 5′-tgcagaggatgattgctgac-3′, reverse 5′-gatcagctcgggcactttag-3′; FasL, forward 5′-catcacaaccactcccagtg-3′, reverse 5′-gttctgccagttccttctgc-3′; Fas, forward 5′-tgtgaacatggaacccttga-3′, reverse 5′-ttcagggtcatcctgtctcc-3′; p53, forward 5′-agagaccgccgtacagaaga-3′, reverse 5′-ctgtagcatgggcatccttt-3′; Foxp3, forward 5′-ctaccccactgctggcaaat-3′, reverse 5′-aggtgaaaggggtcgcata-3′;

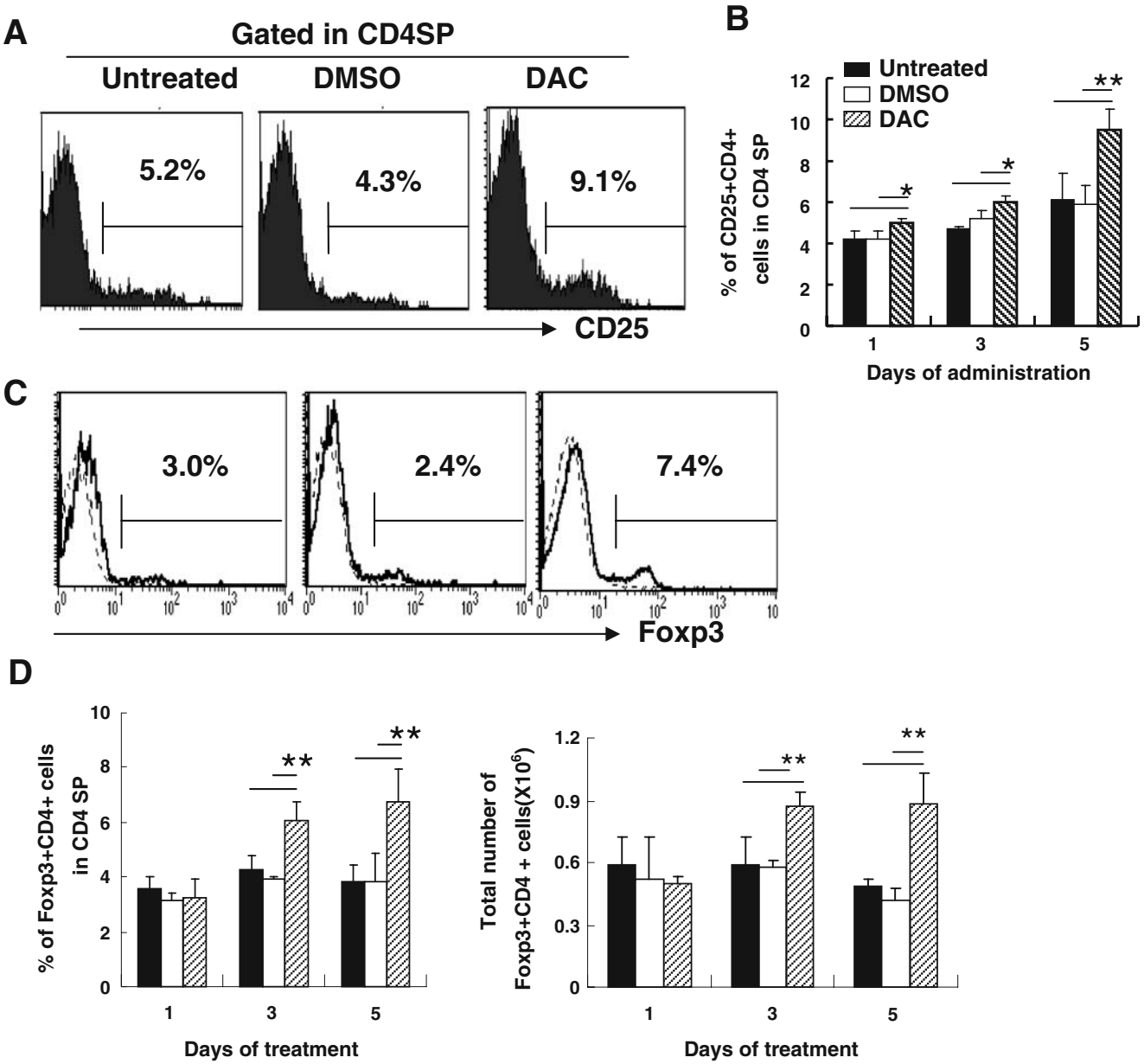

Fig. 3 The significantly enhanced percentage of $CD25^+CD4$ SP cells and total number of $Foxp3^+CD4$ SP Treg cells in the thymus of DAC-treated mice Thymocytes from control and DAC-treated mice were stained with PE-Cy5-labeled anti-CD4 mAb, FITC-labeled anti-CD8 mAb, and PE-labeled anti-CD25 mAb or PE-labeled anti-Foxp3 mAb and analyzed by FCM. **a** One representative of CD25 staining in CD4 SP thymocytes of control and DAC-treated mice. **b** The percentage of $CD25^+$ cells in CD4 SP thymocytes in control and DAC-treated mice are summarized. **c** One representative of Foxp3 staining in CD4 SP thymocytes of control and DAC-treated mice. The *broken* and *solid lines* represent isotype control and specific mAb, respectively. **d** The percentage of $Foxp3^+$ cells in CD4 SP thymocytes and the total number of $Foxp3^+CD4$ SP cells in control and DAC-treated mice are summarized. Results were shown as mean ± SD (N=5), which is one representative of three independent experiments. *p<0.05, **p<0.01 compared with the indicated groups

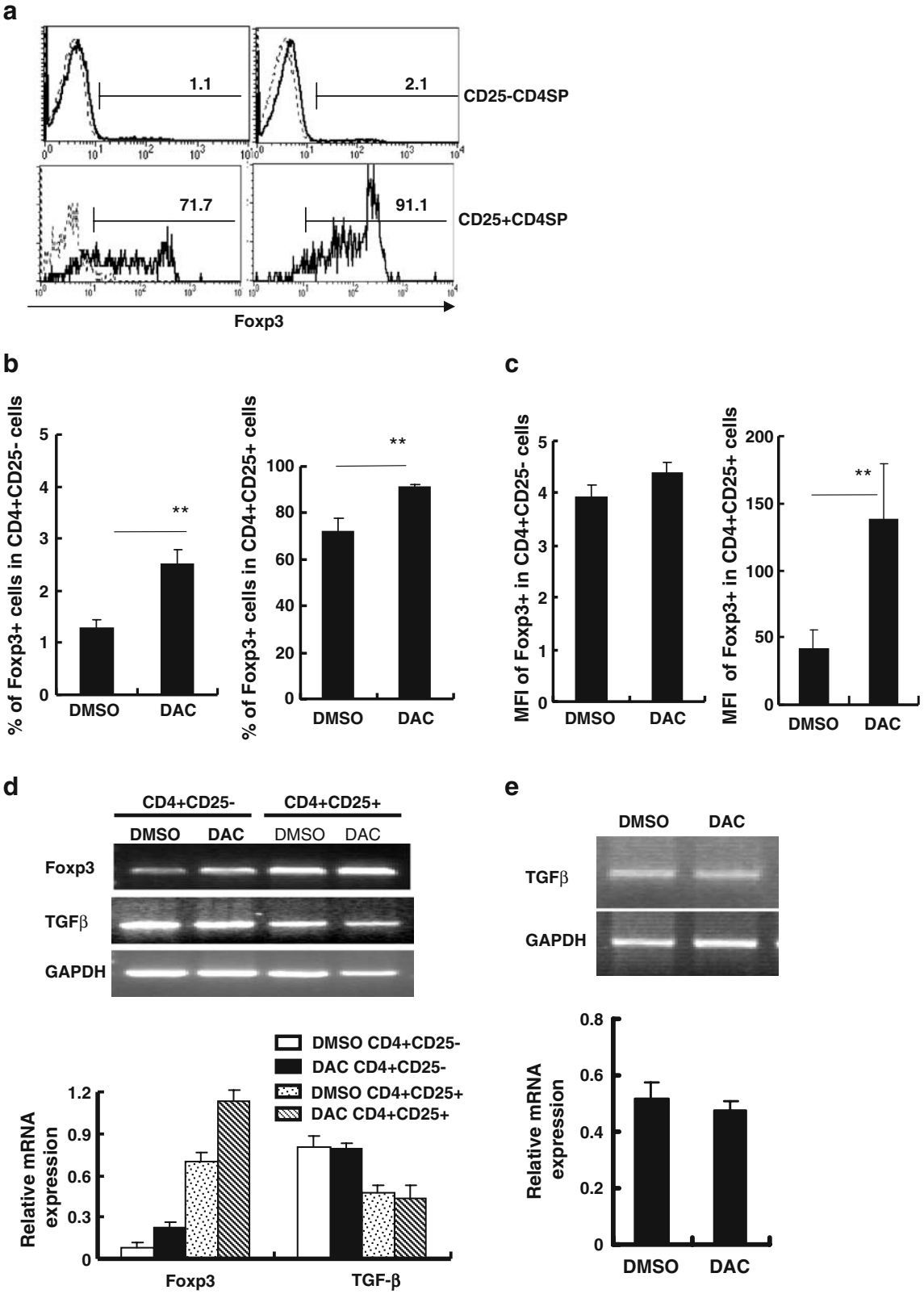
a
1.1
2.1
CD25-CD4SP
71.7
91.1
CD25+CD4SP
Foxp3
b
% of Foxp3+ cells in CD4+CD25- cells
DMSO
DAC
**
% of Foxp3+ cells in CD4+CD25+ cells
c
MFI of Foxp3+ in CD4+CD25- cells
MFI of Foxp3+ in CD4+CD25+ cells
d
CD4+CD25-
CD4+CD25+
Foxp3
TGFβ
GAPDH
DMSO CD4+CD25-
DAC CD4+CD25-
DMSO CD4+CD25+
DAC CD4+CD25+
Relative mRNA expression
TGF-β
e

◀ **Fig. 4** Increased Foxp3$^+$cells in CD25$^-$CD4 SP and CD25$^+$CD4 SP cells in mice treated with DAC. The CD8$^+$ thymocytes were first deleted as described in the "Materials and methods" section, Foxp3$^+$ cells were analyzed in CD25$^-$CD4 SP cells and CD25$^+$CD4 SP cells in DMSO and DAC-treated mice by three-color staining. **a** One representative of Foxp3$^+$ staining in CD25$^-$CD4 SP cells and CD25$^+$CD4 SP cells, the *broken* and *solid lines* represent isotype control and specific mAb, respectively. **b** The percentages of Foxp3$^+$ cells in CD25$^-$CD4 SP cells and CD25$^+$CD4 SP cells in DMSO and DAC-treated mice. **c** The MFI of Foxp3 in CD25$^-$CD4 SP cells and CD25$^+$CD4 SP cells in DMSO and DAC-treated mice. Results were shown as mean ± SD (N=5), which is one representative of three independent experiments. *MFI* median fluorescence intensity. **d** RT-PCR analysis of Foxp3 and TGF-β mRNA expression in CD25$^-$CD4 SP cells and CD25$^+$CD4 SP cells of each group, expressions of Foxp3 and TGF-β mRNAs were semi-quantitatively analyzed by comparing the gray scale of GAPDH, which is one representative of two independent experiments. **e** RT-PCR analysis of TGF-β mRNA expression in thymus of each group, expression of TGF-β mRNAs was semi-quantitatively analyzed by comparing the gray scale of GAPDH

TGFβ, forward 5′- ctcccactcccgtggcttcta -3′, reverse 5′-gttccacatgttgctccacactgg-3; GAPDH, forward 5′-cggcaaatt caacggcacag-3′, reverse 5′-ggatgcagggatgatgttctg-3′.

Purification of mouse thymic CD25$^+$CD4 SP, CD25$^-$CD4 SP cells and splenic CD4$^+$CD25$^+$, CD4$^+$CD25$^-$ cells Thymic CD8$^+$ cells were deleted by anti-mCD8 mAb and complement. CD4$^+$CD25$^+$ and CD4$^+$CD25$^-$ T cells from CD8$^+$ cell-depleted thymocytes and spleen cells were sorted by a FACS DIVA. The purity for CD4$^+$CD25$^+$ and CD4$^+$CD25$^-$ cells was more than 99% in each experiment, respectively. Purified cells were suspended in complete RPMI 1640 medium.

Proliferation assay of T cells to Con A CD25$^-$CD4 SP thymocytes (4×10^4cells/well) were cultured in U-bottom, 96-well plates with syngeneic accessory cells (4×10^4 splenocytes/well, pretreated with 30 μg/ml mitomycin C at 37°C for 30 min), 2 μg/ml Con A and the indicated numbers of syngeneic CD25$^+$CD4SP thymocytes or spleen CD4$^+$CD25$^+$ T cells isolated from either DMSO- or DAC-treated mice for 72 h at 37°C, 5% CO_2. 0.5 μCi [^{3}H] thymidine (185 GBq/mmol) was added to each well for the last 12 h. Cells were harvested onto glass fiber filters with an automatic cell harvester (Tomtec, Toku, Finland). Samples were assayed in a liquid scintillation analyzer (Beckmon Instruments, America). Values are presented as counts per minute (cpm) of triplicate wells.

Methylation assay DNA from thymic CD25$^+$CD4 SP or CD25$^-$CD4 SP cells and splenic CD4$^+$CD25$^+$ or CD4$^+$CD25$^-$ cells were treated with bisulfite as previously described [26]. The denatured DNA was purified by Qiaquick gel extraction kit (Qiagen) and used for PCR. Primers for amplifying the *Foxp3* CpG island region in intron 1 were: forward 5′-ttttggttttttggtatttaaga-3′, reverse 5′-ttaaccaaatttttctaccattaac-3′; Primers for amplifying the *Foxp3* promoter region were: forward 5′-tttgtggtgaggggaa gaaa-3′, reverse 5′-aaaaactaccacattatcaaaaacaa-3′. Primers for amplifying the *H19* gene were: forward 5′- agtattttagggg ggttataaatg-3′, reverse 5′-acccataacataaaatcataaaa-3′. The PCR products were gel extracted (Qiagen) and ligated into a pGEM-T Easy vector by using the TA cloning system (Promega). At least ten separate clones were chosen for sequencing analysis.

Histology Mice were sacrificed and pancreas were dissected and immediately fixed in 4% paraformaldehyde. Paraffin-embedded 10 um sections were stained with hematoxylin and eosin (H&E) and examined under light microscope.

Statistical analysis All data is presented as the mean ± SD. Student's unpaired t test was used to compare groups. P value of less than 0.05 was considered to be statistically significant.

Results

Significant changes in cell number and composition of thymocytes in DAC-treated mice

We first observed the weight, cell number, and composition of thymus in DAC-treated mice. As shown in Fig. 1a, after treatment with DAC at a low dose (0.15 mg/kg, ip) for 1, 3, or 5 days, the weight of thymus and the total cell number of thymocytes decreased continuously. We also observed that the frequency of CD4$^+$CD8$^+$ (DP) population in thymus was markedly reduced after treatment with DAC for 5 days. The frequencies of CD4 SP, CD8 SP, and CD4$^-$CD8$^-$ (DN) populations were increased concomitantly in the thymi of DAC-treated mice (Fig. 1b and c). However, the absolute numbers of DP, CD4 SP and DN cells were decreased significantly while the absolute number of CD8 SP cells did not show significant change (Fig. 1d).

No increased apparent cell cycle arrest and apoptosis of thymocytes were detectable in DAC-treated mice

Thymocytes are specifically susceptible to apoptosis during TCR repertoire selection in response to hormonal signals and DNA damage [27–29]. We therefore examined the changes of cell cycle and apoptosis of thymocytes in response to DAC treatment for 5 days. No significant changes of cell cycle distribution were observed in the total thymocytes of DAC-treated mice compared with DMSO-

treated mice (Fig. 2a and b). In addition, we measured the apoptosis in thymocytes by Annexin V/PI staining. Though the apoptosis of total thymocytes including early phase apoptotic cells (Annexin V^+PI^-) and late phase apoptotic cells (Annexin V^+PI^+) was higher in DAC-treated mice than in DMSO-treated mice, there was no statistical difference ($P>0.05$, Fig. 2c and d). The expression of apoptosis or DNA damage-related genes, such as Bad, Bax, FasL, Fas, and p53, were decreased in DP cells (FasL, Fas, and p53), CD4 SP cells (Bad, Bax, Fas, and p53) and total thymocytes (p53 and Fas) in DAC-administrated mice as determined by RT-PCR analysis (Fig. 2e and Supplemental Fig. 1).

Significantly enhanced percentage of $CD25^+$CD4 SP cells and total number of $Foxp3^+$CD4 SP cells in the thymi of DAC-treated mice

It is well known that the majority of natural $CD4^+CD25^+$ $Foxp3^+$ Treg cells are produced in the thymus [13, 30, 31]. To assess the effect of DAC on $CD25^+$CD4 SP cells in the thymus, we compared the percentages and cell numbers of $CD25^+$CD4 SP cells and $Foxp3^+$CD4 SP cells in the DAC-treated mice to those in control mice. The percentage of $CD25^+$CD4 SP cells increased even 1 day after DAC treatment and continuously increased until 5 days (Fig. 3a and b), while the total number of $CD25^+$CD4 SP cells did not show detectable change (data not shown). In contrast, both the percentage and the total number of $Foxp3^+$CD4 SP cells increased significantly after DAC treatment for 3 days (Fig.3c and d). Therefore, DAC treatment can significantly increase the percentages of $CD25^+$CD4 SP cells and, importantly, the total number of $Foxp3^+$CD4 SP cells in the thymus. However, the short-term treatment with DAC did not change the peripheral $CD25^+CD4^+$ Treg cells in mice (Supplemental Fig. 2).

Increased proportion of $Foxp3^+$ cells in $CD25^-$CD4 SP cells and $CD25^+$CD4 SP cells in mice treated with DAC

DAC treatment leads to increased number of $Foxp3^+$CD4 SP cells in the thymus. We wondered whether $CD25^-$CD4 SP cells and $CD25^+$CD4 SP cells acquired similar Foxp3 expression after DAC treatment. We depleted $CD8^+$ thymocytes and analyzed the Foxp3 expression in $CD25^-$CD4 SP cells and $CD25^+$CD4 SP cells by flow cytometric analysis. As shown in Fig. 4a and b, increased proportion of $Foxp3^+$ cells in both $CD25^-$CD4 SP cells and $CD25^+$CD4 SP cells were observed in DAC-treated mice compared to DMSO-treated mice. In addition, MFI of Foxp3 increased significantly in $CD25^+$CD4 SP cells but not in $CD25^-$CD4 SP cells (Fig. 4c), since TGF-β plays an important role in the induction of Foxp3 expression, we detected whether TGF-β is involved in the DAC-induced Foxp3 expression. As shown in Fig. 4d and e, although messenger RNA encoding Foxp3 increased in both $CD25^-$CD4 SP cells and $CD25^+$CD4 SP cells in DAC-treated mice, no significant increase of TGF-β expression in $CD25^-$CD4 SP cells, $CD25^+$CD4 SP cells, and thymus tissue in DAC-treated mice was detected (Supplemental Fig. 3). So, the increased expression of Foxp3 induced by DAC treatment in $CD25^+$CD4 SP cells was likely independent of the induction of TGF-β in the thymus.

Phenotype changes of $CD25^+$CD4 SP cells and $CD25^-$CD4 SP cells in mice with DAC treatment

$CD4^+CD25^+$ Treg cells express diverse surface molecules, including cytotoxic lymphocyte antigen-4 (CTLA-4), glucocorticoid-induced tumor necrosis factor receptor family-related gene (GITR) and so on. In addition, high expression of CD5 and low expression of CD45RB were used to enrich for the Treg cell population [32]. To further characterize the phenotypes of $CD25^+$CD4 SP and $CD25^-$CD4 SP thymocytes in DAC-treated mice, we detected the expression of several cell surface molecules including CTLA-4, GITR, CD45RB, and CD62L. As shown in Fig. 5a and b, the proportion of CTLA-4, GITR, and CD62L positive cells increased significantly in $CD25^+$CD4 SP cells in DAC-treated mice. The proportions of CTLA-4 and CD62L positive cells increased in $CD25^-$CD4 SP cells in DAC-treated mice as well. However, the proportion of $CD45RB^+$ cells was decreased significantly in $CD25^+$CD4SP cells in DAC-treated mice. Identically, MFI of CTLA-4 and CD62L increased significantly in both $CD25^+$CD4 SP cells and $CD25^-$CD4 SP cells in DAC-treated mice, while MFI of CD45RB decreased significantly in $CD25^+$CD4 SP cells in DAC-treated mice (Fig. 5c).

Enhanced immunosuppressive function of $CD25^+$CD4 SP thymocytes in DAC-treated mice

To assess whether DAC treatment might interfere with the function of Treg cells, we first sorted $CD4^+CD25^+$ Treg cells from both thymus and spleen in mice treated with DAC or DMSO, and then compared their immunosuppressive function by measuring the proliferation of $CD25^-$CD4 SP effector cells in vitro[25, 33]. As shown in Fig. 6a, with the increased ratios of $CD25^+$CD4 SP thymocytes to $CD25^-$CD4 SP effector cells, $CD25^+$CD4 SP thymocytes from either DMSO or DAC-treated mice showed an enhanced suppressive ability on the proliferation of $CD25^-$CD4 SP effector cells induced by mitogen Con A. Importantly, the immunosuppressive ability of thymic Treg cells in DAC-treated mice was stronger than that in DMSO-treated mice. In addition, splenic $CD4^+CD25^+$ cells from

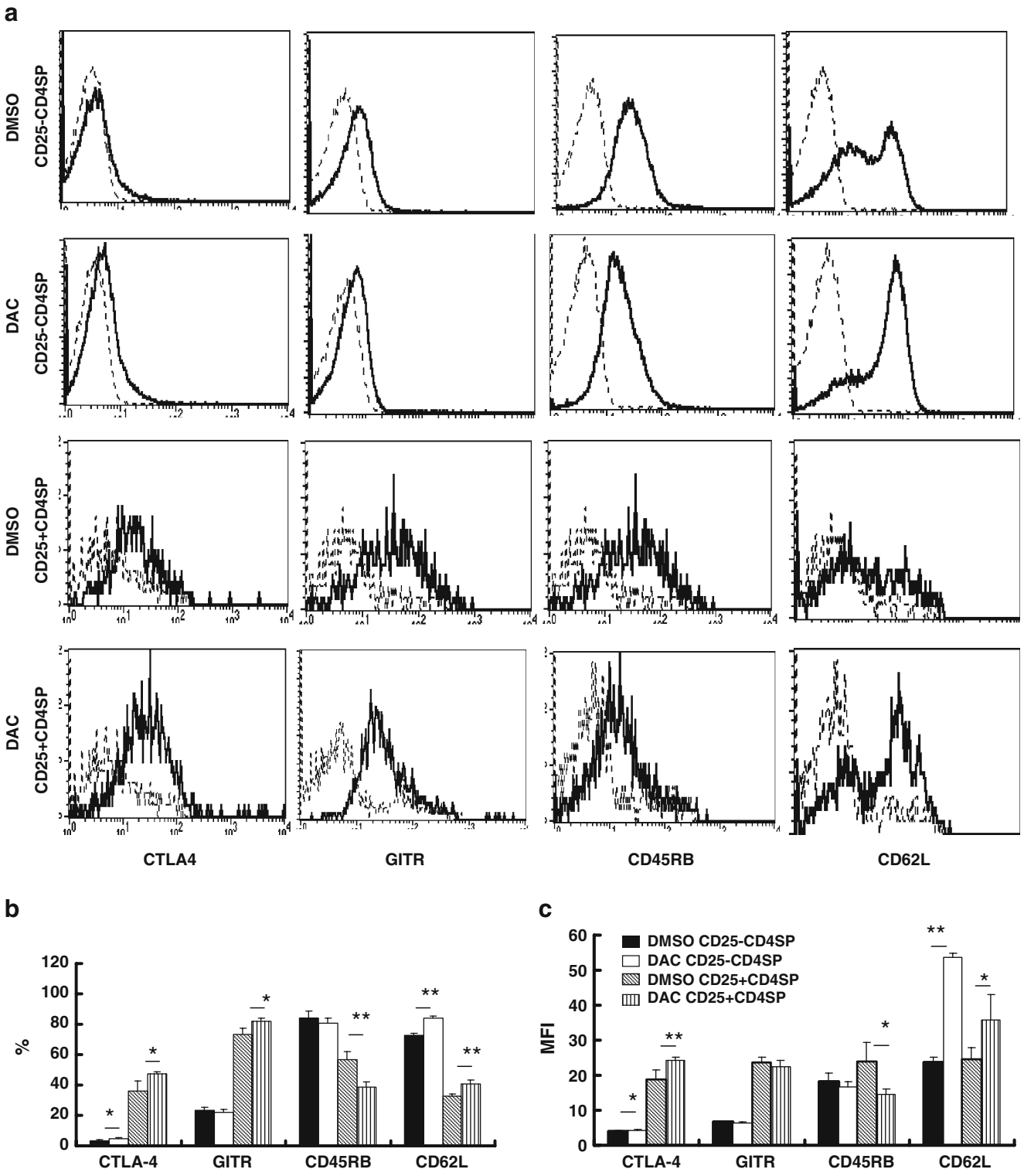

Fig. 5 Phenotype changes of $CD25^{-}$CD4 SP and $CD25^{+}$CD4 SP cells in mice treated with DAC. The $CD8^{+}$ thymocytes were first deleted as described in materials and methods, cell surface molecules including CTLA-4, GITR, CD45RB, and CD62L were analyzed in $CD25^{-}$CD4 SP cells and $CD25^{+}$CD4 SP cells by three-color staining. **a** One representative of CTLA-4, GITR, CD45RB, and CD62L staining in $CD25^{-}$CD4 SP cells and $CD25^{+}$CD4 SP cells in DMSO and DAC-treated mice. The *broken* and *solid lines* represent isotype control and specific mAb, respectively. **b** The percentages of CTLA-4^{+}, $GITR^{+}$, $CD45RB^{+}$, and $CD62L^{+}$ cells in $CD25^{-}$CD4 SP cells and $CD25^{+}$CD4 SP cells in DMSO and DAC-treated mice are summarized. **c** The MFI of CTLA-4, GITR, CD45RB, and CD62L in $CD25^{-}$CD4 SP cells and $CD25^{+}$CD4 SP cells in DMSO and DAC-treated mice are summarized

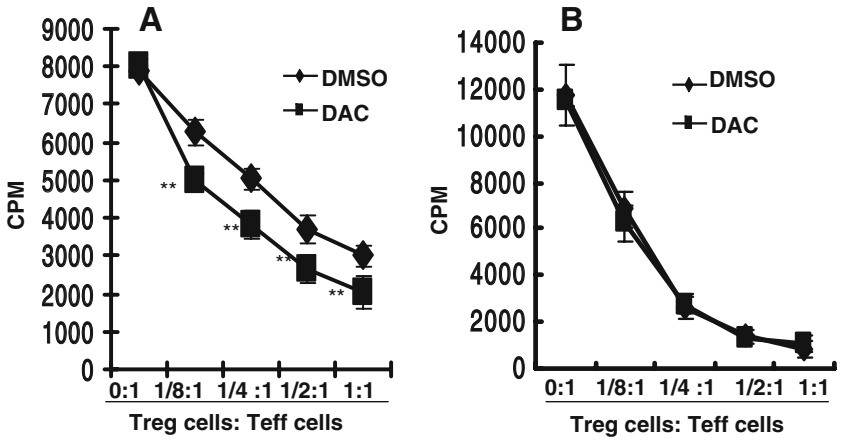

Fig. 6 Enhanced immunosuppressive function of $CD25^+CD4$ SP cells in DAC-treated mice. The immunosuppressive function of $CD25^+CD4$ SP cells and spleen $CD4^+CD25^+$ T cells was determined using the traditional in vitro assay. **a** Both $CD25^+CD4$ SP cells in DMSO and DAC-treated mice inhibited the proliferation of $CD25^-CD4$ SP effector cells to mitogen Con A. However, $CD25^+CD4$ SP cells from DAC-treated mice exhibited a significantly higher immunosuppressive function than that of $CD25^+CD4$ SP cells from DMSO-treated mice at the same dose (**$P<0.01$). **b** Splenic $CD4^+CD25^+$ Treg cells in both DMSO and DAC-treated mice inhibited the proliferation of $CD4^+CD25^-$ effector cells to mitogen Con A, while no significant difference of suppressive ability was observed between these two groups. Data are shown as mean ± SD, which is one representative of two independent experiments

both DMSO- and DAC-treated mice could efficiently suppress the proliferation of $CD25^-CD4$ SP effector cells without detectable difference (Fig. 6b). These data indicate that the short-term treatment with DAC changed thymic but not splenic $CD4^+CD25^+$ Treg cells in mice.

Reduced *Foxp3* intron 1 methylation in $CD25^+CD4$ SP cells in DAC-treated mice

It is well known that DAC induces gene expression through DNA demethylation [34–36]. We wonder whether a demethylated *Foxp3* gene could be observed in $CD25^-CD4$ SP cells or $CD25^+CD4$ SP cells in DAC-treated mice. A CpG island in the +4,393 to +4,506 region of the *Foxp3* intron 1 and a promoter region from −250 to +1 of the *Foxp3* gene were selected for the methylation analysis (Fig. 7a and Supplemental Fig. 4A). Purified $CD25^+CD4$ SP cells and $CD25^-CD4$ SP cells were sorted from DAC-treated and control male mice (Fig. 7b). Male mice were chosen to avoid potential artifacts due to random X chromosome inactivation since Foxp3 is encoded on the X chromosome [37]. In addition, to compare the methylation status of *Foxp3* in thymus to those in periphery, splenic $CD4^+CD25^+$ cells and $CD4^+$ $CD25^-$ cells were sorted for this assay, too. As shown in Fig. 7c, the $CD4^+CD25^-$cells from both spleen and thymus displayed an almost complete methylation in the CpG island of Foxp3 intron1 (98% vs 98%). In contrast, the CpG island of Foxp3 intron1 was partially methylated in thymic $CD25^+CD4$ SP cells while almost completely unmethylation was observed in splenic $CD4^+CD25^+$ cells from the control mice (methylation in thymic $CD25^+CD4$ SP cells and splenic $CD4^+CD25^+$ cells was 46% vs. 1%). A remarkable demethylation of this CpG island was observed in the $CD25^+CD4$ SP thymocytes in DAC-treated mice (46% to 33%), while only a slight demethylation of this *Foxp3* locus was observed in $CD25^-CD4$ SP thymocytes in DAC-treated mice (98% to 94%). The promoter region of *Foxp3* displayed a partial methylation status in $CD25^-CD4$ SP thymocytes, but little methylation in $CD25^+CD4$ SP thymocytes in DMSO-treated mice (42% vs 4%). DAC treatment resulted in a 9% demethylation in the promoter region of *Foxp3* in $CD25^-CD4$ SP thymocytes (42% to 33%; Table 1 and Supplemental Fig. 4B). To explore the specificity of the demethylation in the Foxp3 gene affected by DAC treatment, we also measured the methylation status of the H19 gene which is a paternally imprinted gene and whose methylation is modulated during oogenesis and spermatogenesis [38]. As shown in Table 1 and Supplemental Fig. 4c, *H19* gene exhibited little demethylation in both $CD25^-CD4$ SP and $CD25^+CD4$ SP thymocytes in DAC-treated mice compared with that in DMSO-treated mice. Therefore, the induction of thymic $CD4^+CD25^+$ Treg cells in DAC-treated mice is likely due to the augmentation of Foxp3 gene expression through *Foxp3* intron 1 demethylation.

DAC administration significantly prevented the occurrence of type 1 diabetes in CY-NOD mice

To determine whether DAC administration might play a role in the therapy of autoimmune disease, we employed NOD mice as recipients which were treated with DAC at a low dose (0.1 mg/kg) for 5 weeks. To accelerate the development of diabetes, NOD mice were injected with

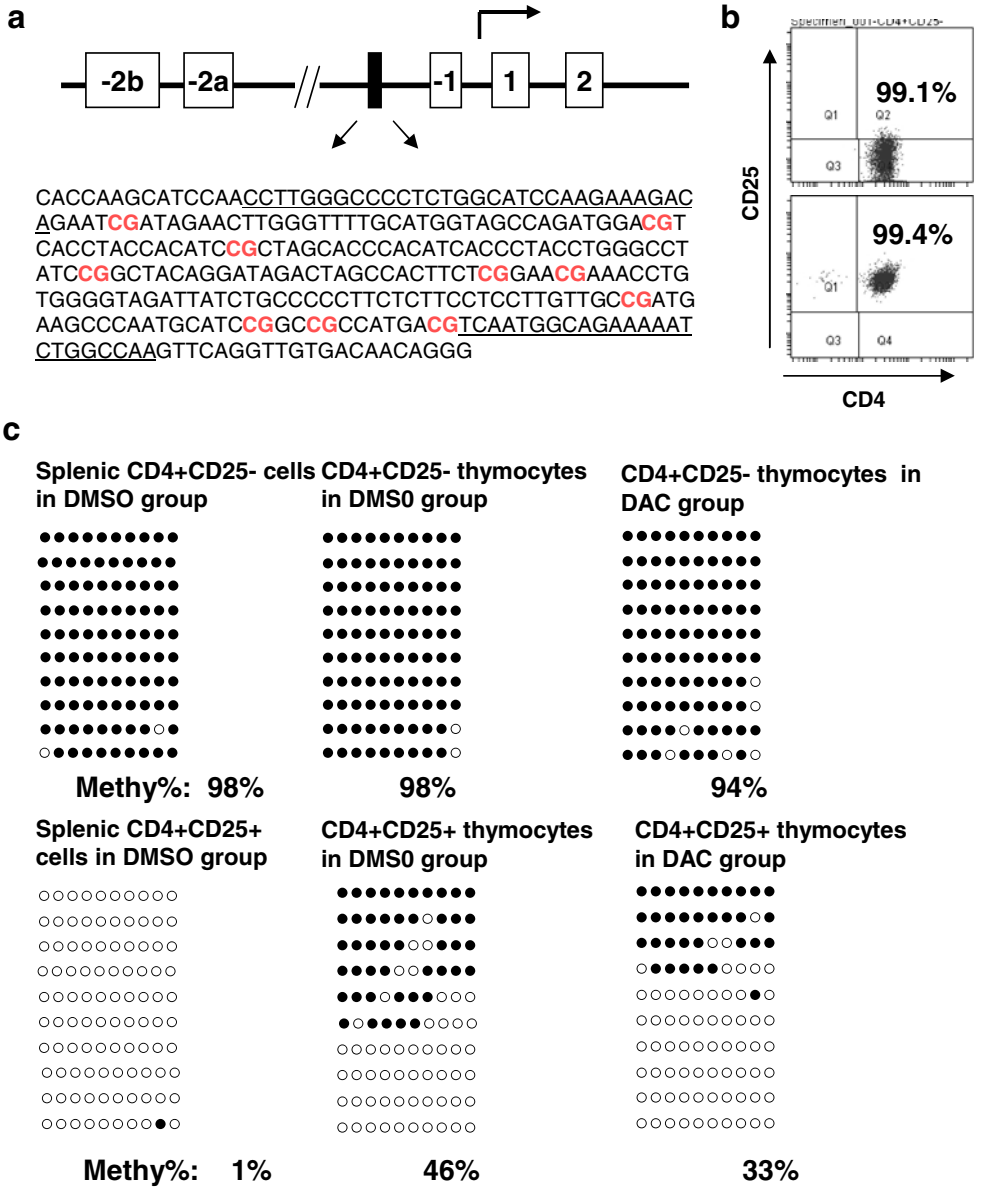

Fig. 7 Reduced *Foxp3* methylation in CD25$^+$CD4 SP cells in DAC-treated mice. **a** Schematic view of mouse *Foxp3* gene and the position of selected CpG island in intron1. Distribution and position of individual CpG motifs within the selected CpG island are shown bellow, individual CpG motifs are shown in bold letters. *Arrow* represents putative transcription start site and targets for primers design are *underlined*. **b** Representative FACS samples demonstrating the sorting purities of CD25$^+$CD4 SP cells and CD25$^-$CD4 SP cells. *Numbers* in the dot-plot indicate the purity of sorted CD25$^+$CD4 SP cells or CD25$^-$CD4 SP cells. **c** Bisulfite sequencing of the selected CpG island in the *Foxp3* intron 1. This sequence spans 259 bp and includes ten CpGs. Genomic DNA was isolated from the indicated T cell subsets, modified with sodium bisulfite, PCR amplified, cloned into the pGEM-T vector, and individual clones were sequenced. The methylation pattern of each clone obtained is shown. *filled circle* methylated CpG, *empty circle* nonmethylated CpG. The percentages of mCpGs in total CpGs for each group are presented below the diagram

cyclophosphamide (CY, 250 mg/kg) once at 8 weeks old. As shown in Fig. 8a and b, DAC administration inhibited the occurrence of diabetes in the CY-NOD mice. Twenty percent of the mice in the DMSO-treated NOD group became diabetic at 2 weeks after CY induction, and it increased to 62.5% at 4 weeks after CY induction in the DMSO-treated NOD group. In contrast, none of the DAC-treated NOD mice developed diabetes at 6 weeks after CY induction (Fig. 8b). An apparent lymphocyte infiltration in the islets or lack of complete islets was detected in DMSO-treated mice by histology analysis. However, the islets in the DAC-treated mice displayed no manifest structure destruction or lymphocyte infiltration (Fig. 8c). Comparing the percentage of CD4$^+$CD25$^+$ cells and Foxp3 expression

Table 1 Methylation status of *Foxp3* intron1, promoter and *H19* gene in CD25$^-$CD4SP cells and CD25$^+$CD4SP cells in DMSO- and DAC- treated mice

Treatment	Cell subsets	mCpG %		
		Foxp3 intron 1	*Foxp3* promoter	*H19*
DMSO	CD4+CD25-	98%	42%	58%
DAC	CD4+CD25-	94%	33%	54%
DMSO	CD4+CD25+	46%	4%	61%
DAC	CD4+CD25+	33%	2%	58%

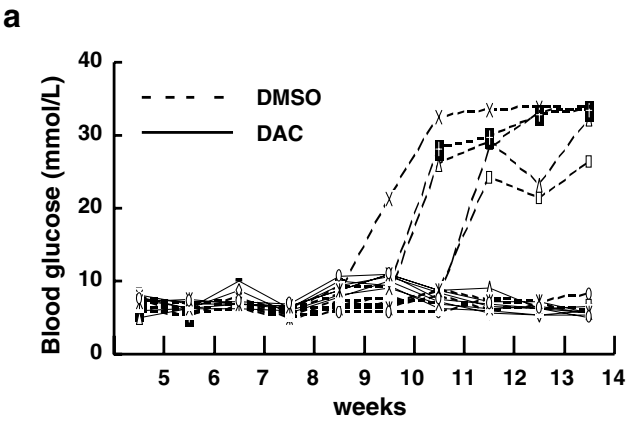
a
Blood glucose (mmol/L)
DMSO
DAC
weeks

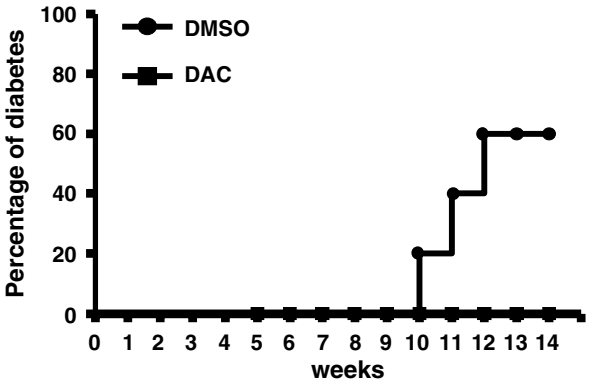
b
Percentage of diabetes
DMSO
DAC
weeks

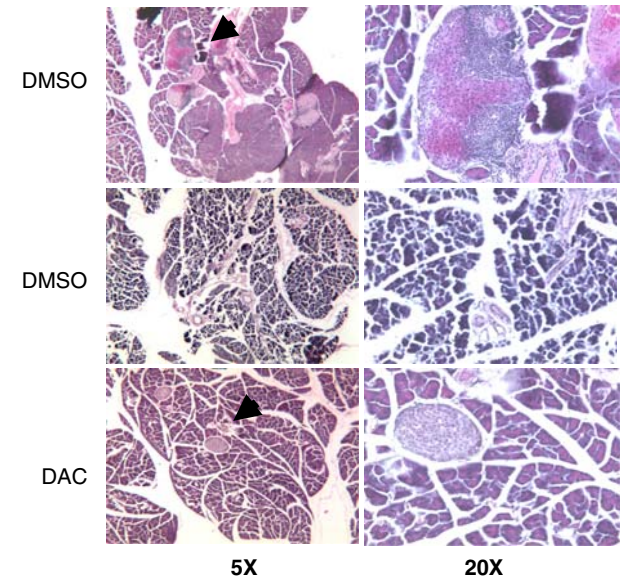
c
DMSO
DMSO
DAC
5X
20X

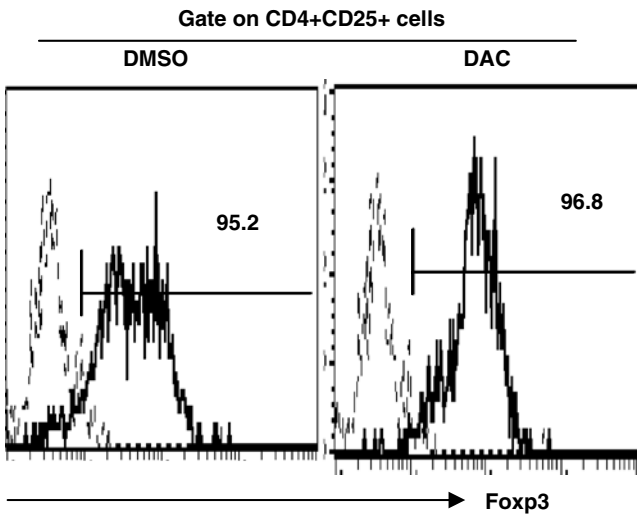
e
Gate on CD4+CD25+ cells
DMSO
DAC
95.2
96.8
Foxp3

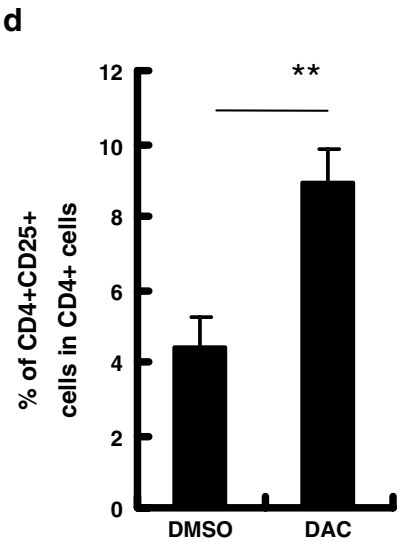
d
% of CD4+CD25+ cells in CD4+ cells
**
DMSO
DAC

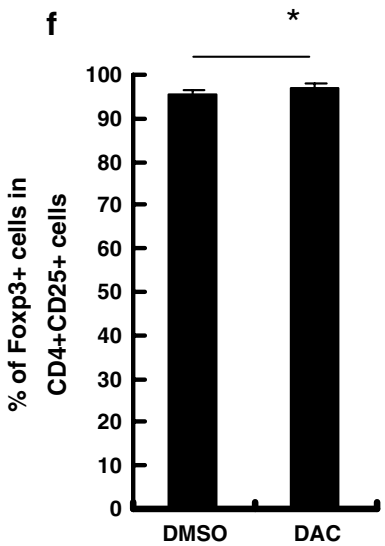
f
% of Foxp3+ cells in CD4+CD25+ cells
*
DMSO
DAC

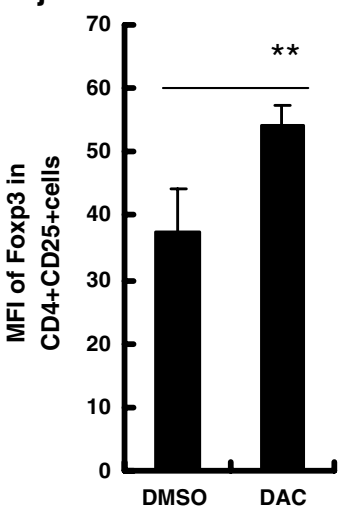
j
MFI of Foxp3 in CD4+CD25+cells
**
DMSO
DAC

◀ **Fig. 8** DAC treatment significantly prevented the development of type 1 diabetes in CY-NOD mice. **a** Blood glucose in NOD mice treated with or without DAC. 5-week-old NOD mice were injected with DAC (0.1 mg/kg) every day for a total of 5 weeks, diabetes was inducted by CY (250 mg/kg) injection at 8 weeks old. The level of blood glucose of each NOD mice in DMSO or DAC-treated group was measured weekly. **b** DAC treatment significantly prevented the development of type 1 diabetes in CY-NOD mice. Diabetes was affirmed when the blood glucose was over 11.1 mM. **c** At 6 weeks after CY induction, islets were examined by H&E staining. The staining images were given at 5 and 20 magnifications; islets were pointed by arrows at 5 magnification images. **d** The percentage of $CD4^+CD25^+$ cells in $CD4^+$ cells of DMSO and DAC-treated CY-NOD mice are summarized. **e** One representative of Foxp3 staining $CD4^+CD25^+$ cells of DMSO and DAC-treated CY-NOD mice. The *broken* and *solid lines* represent isotype control and specific mAb, respectively. **f** The percentage of $Foxp3^+$ cells in $CD4^+CD25^+$ cells of DMSO and DAC-treated CY-NOD mice are summarized. **j** The MFI of Foxp3 in $CD4^+CD25^+$ cells of DMSO and DAC-treated CY-NOD mice are summarized

in the PBL of DAC-treated CY-NOD mice to those in control mice, we found that the percentage of $CD4^+CD25^+$ cells was significantly increased in $CD4^+$ T cells in DAC-treated CY-NOD mice as compared with those from DMSO-treated CY-NOD mice ($P<0.01$, Fig. 8d). In addition, the percentage of $Foxp3^+$ cells and MFI of Foxp3 increased significantly in $CD4^+CD25^+$ cells from DAC-treated CY-NOD mice (Fig. 8e and f). Thus, DAC administration prevented the occurrence of type 1 diabetes in CY-NOD mice, which is probably due to the increased percentage of $CD4^+CD25^+$ cells in peripheral $CD4^+$ cells and up-regulation of Foxp3 in $CD4^+CD25^+$ cells in DAC-treated NOD mice.

Discussion

As a classical DNA demethylation agent, DAC is widely used in cancer models and patients; however, little is known about the effects of DAC on T lymphocytes especially $CD4^+CD25^+$ Treg cells. In the present study, we found that treatment with DAC at a low dose (1.5 mg/kg/day, ip) for a short time remarkably increased the percentage and number of $Foxp3^+$ Treg cells in the thymus in mice. Furthermore, DAC could induce a significant demethylation of the CpG island in the first intron of the *Foxp3* gene in the $CD25^+CD4SP$ thymocytes. These observations suggest that epigenetic regulating events are closely involved in the development of $Foxp3^+$ Treg cells in thymus.

DAC significantly enhanced the percentages of thymic $CD25^+CD4SP$ cells and $Foxp3^+CD4SP$ cells. Increased ratio of $CD25^+CD4SP$ to $CD25^-CD4SP$ cells in the thymi of DAC-treated mice may be resulted from the different resistance to apoptosis induced by DAC between $CD25^-CD4SP$ cells and $CD25^+CD4SP$ cells. It is reported that $CD4^+CD25^-$ cells are more prone to apoptosis than $CD4^+CD25^+$ Treg cells in stress conditions [33, 39]. Importantly, the total number of $Foxp3^+CD4SP$ cells in the thymus increased significantly after DAC treatment, though the total number of $CD25^+CD4SP$ cells remains unchanged. These data indicate that a low dose of DAC treatment did not affect the proliferation or apoptosis of $CD25^+CD4SP$ cells, but up-regulate the expression of Foxp3 in CD4SP cells. This speculation is further supported by the observation that dramatically increased percentage of $Foxp3^+$ cells and enhanced Foxp3 expression concurrently occurred in $CD25^+CD4SP$ cells in DAC-treated mice. Comparing with peripheral $CD25^+CD4^+$ Treg cells, in which the CpG motifs within the CpG island of *Foxp3* intron 1 were almost completely demethylated (99%), $CD25^+CD4SP$ thymocytes showed a clearly reduced degree of demethylation of the *Foxp3* gene (54%). However, after the treatment with DAC, $CD25^+CD4SP$ thymocytes showed a significantly increased degree of demethylated CpG motifs within the CpG island of *Foxp3* first intron (67%). On the other hand, even through Foxp3 is not expressed in $CD25^-CD4SP$ cells, less than half of the CpG sites in the promoter region of *Foxp3* gene were methylated (42%, Supplemental Fig. 1) , while almost all CpG sites in the intronic region of *Foxp3* gene were methylated in $CD25^-CD4SP$ cells (98%), indicating Foxp3 expression is inversely correlated with the methylation status of the intronic CpG island of the *Foxp3* gene, while demethylation of the promoter region of *Foxp3* had relatively slight effect on foxp3 expression, as previously reported [19].

Using Foxp3-GFP knockin mice, Fontenot et al. found that "would-be" Treg cells or Treg precursors that have a $CD4^+CD25^+Foxp3^-$ phenotype exist in the thymus [9, 12]. Natural $CD4^+CD25^+$ Treg cells developed in the thymus through interactions with self-peptide–MHC complexes and transiently activated (high expression of CD25) before acquiring full mature phenotypes and suppressive function [40–43]. Actually, in addition to the induction of Foxp3 expression in $CD4^+CD25^+$ thymocytes, DAC treatment up-regulated the expression of GITR, CTLA-4, and CD62L as well as down-regulated the expression of CD45RB significantly in $CD4^+CD25^+$ thymocytes. Taken together, DNA demethylation may play a critical role during the phenotype maturation of $CD4^+CD25^+Foxp3^+$ Treg cells.

$CD4^+CD25^+$ thymocytes in DAC-treated mice showed increased immunosuppressive ability as determined in an in vitro traditional assay. More importantly, DAC in vivo treatment significantly inhibited the development of type 1 diabetes in CY-NOD mice, as well as reduced lymphocyte infiltration in islets and enhanced percentage of peripheral $CD4^+$ $CD25^+$ Treg cells in $CD4^+$ cells of DAC-treated CY-NOD mice. Thus, DNA demethylation may have a clinical therapeutic effect on autoimmune disease. However, it is unclear whether the enhanced immunosuppressive ability of

$CD4^+$ $CD25^+$ Treg cells is due to the enhanced percentage of $Foxp3^+$ cells in $CD4^+$ $CD25^+$ Treg cells, the enhanced Foxp3 expression in each cells, or cell phenotype alternation. It is likely that all these changes may contribute to the enhanced immunosuppressive function of $CD4^+$ $CD25^+$ Treg cells isolated from DAC-treated mice. It should be clarified in the coming studies.

Though the changes of $Foxp3^+$ Treg cells in the thymi of DAC-treated mice were striking, no significantly enhanced Foxp3 expression and no conversion of $CD4^+CD25^-$ T cells to $Foxp3^+$ Treg cells were observed in peripheral lymphoid tissues in mice after DAC treatment for 5 days (Supplemental Fig. 1). Accordingly, no enhanced immunosuppressive ability of peripheral $CD4^+CD25^+$ Treg cell in DAC-treated mice was observed (Fig. 6b). These data collectively indicate that thymic $Foxp3^+$ Treg cell development may be more sensitive to DNA demethylation than peripheral induction of $Foxp3^+$ Treg cells in naïve mice. It is reported that inhibiting methylation with 5-azacytidine induces obvious Foxp3 expression during mature $CD4^+CD25^-$ T cell activation in vitro [19, 21]. The inconsistency with our observation showing that the short-term treatment with a low dose of DAC did not remarkably induce Foxp3 expression in peripheral $CD4^+CD25^-$ T cells in mice may be due to the different experimental systems, such as the in vitro and the in vivo assays, or the duration of the treatment. However, long-term treatment with DAC increased the percentages of peripheral $CD4^+CD25^+$ Treg cells in NOD mice, indicating that DAC does affect the peripheral $CD4^+CD25^+$ Treg levels. Furthermore, our preliminary study showed that the in vitro treatment with DAC significantly induced Foxp3 expression in $CD4^+CD25^+$ cells from both spleen and thymus during activation without detectable difference (Supplemental Fig. 5). The different effect of DAC on peripheral and thymic $CD4^+CD25^+$ Treg development in vivo and in vitro needs to be determined.

Treatment with a low dose of DAC remarkably reduced the cell number of thymocytes which is consistent with previous reports [44–46]. Interestingly, no obvious cell cycle arrest and apoptosis of thymocytes were detected in DAC-treated mice. In addition, RT-PCR analysis of apoptosis-related genes such as Bad, Bax, FasL, Fas, and p53 showed that instead of increase, all of these genes decreased in DP cells or CD4SP cells in DAC-administrated mice. This apparent contradiction to the reduced thymocytes in DAC-treated mice may be explained by the fact that apoptotic thymocytes can be removed efficiently and quickly by thymic phagocytes and the survived cells are more resistant to cell death [47–50].

In conclusion, DAC-induced *Foxp3* demethylation in vivo significantly increased the percentage and cell number of thymic $CD4^+CD25^+Foxp3^+$ Treg cells via enhancing Foxp3 expression in immature $CD4^+CD25^+Foxp3^-$ T cells in thymus indicating that epigenetic regulation is involved in the phenotype and functional maturation of $CD4^+CD25^+Foxp3^+$ Treg cells. Moreover, DAC treatment in CY-NOD mice could significantly inhibit the occurrence of diabetes, supporting that DAC may have potential applications for the treatment of patients with autoimmune diseases.

Acknowledgments The authors wish to thank Ms. Jing Wang and Ms. Jianxia Peng for their expertise technical assistance, Ms. Qinghuan Li for her excellent laboratory management. This work was supported by grants from National Natural Science Foundation (30630060, 30425026, Y.Z.), and the Scientific Research Foundation for the Returned Overseas Chinese Scholars of State Education Ministry (2005-546, Y.Z.).

Conflict of interest statement The authors declare that they have no conflicts of interest.

References

1. Sakaguchi S, Ono M, Setoguchi R, Yagi H, Hori S, Fehervari Z, Shimizu J, Takahashi T, Nomura T (2006) Foxp3+ CD25+ CD4+ natural regulatory T cells in dominant self-tolerance and autoimmune disease. Immunol Rev 212:8–27
2. Maloy KJ, Powrie F (2001) Regulatory T cells in the control of immune pathology. Nat Immunol 2:816–822
3. Watanabe N, Wang YH, Lee HK, Ito T, Wang YH, Cao W, Liu YJ (2005) Hassall's corpuscles instruct dendritic cells to induce CD4+CD25+ regulatory T cells in human thymus. Nature 436:1181–1185
4. Kretschmer K, Apostolou I, Hawiger D, Khazaie K, Nussenzweig MC, von Boehmer H (2005) Inducing and expanding regulatory T cell populations by foreign antigen. Nat Immunol 6:1219–1227
5. Fontenot JD, Gavin MA, Rudensky AY (2003) Foxp3 programs the development and function of CD4+CD25+ regulatory T cells. Nat Immunol 4:330–336
6. Apostolou I, von Boehmer H (2004) In vivo instruction of suppressor commitment in naive T cells. J Exp Med 199:1401–1408
7. Yagi H, Nomura T, Nakamura K, Yamazaki S, Kitawaki T, Hori S, Maeda M, Onodera M, Uchiyama T, Fujii S, Sakaguchi S (2004) Crucial role of FOXP3 in the development and function of human CD25+CD4+ regulatory T cells. Int Immunol 16:1643–1656
8. Hori S, Nomura T, Sakaguchi S (2003) Control of regulatory T cell development by the transcription factor Foxp3. Science 299:1057–1061
9. Fontenot JD, Rasmussen JP, Williams LM, Dooley JL, Farr AG, Rudensky AY (2005) Regulatory T cell lineage specification by the forkhead transcription factor foxp3. Immunity 22:329–341
10. Aarts-Riemens T, Emmelot ME, Verdonck LF, Mutis T (2008) Forced overexpression of either of the two common human Foxp3 isoforms can induce regulatory T cells from CD4(+)CD25(−) cells. Eur J Immunol 38:1381–1390
11. Loser K, Hansen W, Apelt J, Balkow S, Buer J, Beissert S (2005) In vitro-generated regulatory T cells induced by Foxp3-retrovirus infection control murine contact allergy and systemic autoimmunity. Gene Ther 12:1294–1304
12. Lio CW, Hsieh CS (2008) A two-step process for thymic regulatory T cell development. Immunity 28:100–111
13. Itoh M, Takahashi T, Sakaguchi N, Kuniyasu Y, Shimizu J, Otsuka F, Sakaguchi S (1999) Thymus and autoimmunity: production of CD25+CD4+ naturally anergic and suppressive T cells as a key function of the thymus in maintaining immunologic self-tolerance. J Immunol 162:5317–5326

14. Pennington DJ, Silva-Santos B, Silberzahn T, Escorcio-Correia M, Woodward MJ, Roberts SJ, Smith AL, Dyson PJ, Hayday AC (2006) Early events in the thymus affect the balance of effector and regulatory T cells. Nature 444:1073–1077
15. Fontenot JD, Dooley JL, Farr AG, Rudensky AY (2005) Developmental regulation of Foxp3 expression during ontogeny. J Exp Med 202:901–906
16. Wilson CB, Makar KW, Shnyreva M, Fitzpatrick DR (2005) DNA methylation and the expanding epigenetics of T cell lineage commitment. Semin Immunol 17:105–119
17. Floess S, Freyer J, Siewert C, Baron U, Olek S, Polansky J, Schlawe K, Chang HD, Bopp T, Schmitt E, Klein-Hessling S, Serfling E, Hamann A, Huehn J (2007) Epigenetic control of the foxp3 locus in regulatory T cells. PLoS Biol 5:e38
18. Bassuny WM, Ihara K, Sasaki Y, Kuromaru R, Kohno H, Matsuura N, Hara T (2003) A functional polymorphism in the promoter/enhancer region of the FOXP3/Scurfin gene associated with type 1 diabetes. Immunogenetics 55:149–156
19. Kim HP, Leonard WJ (2007) CREB/ATF-dependent T cell receptor-induced FoxP3 gene expression: a role for DNA methylation. J Exp Med 204:1543–1551
20. Polansky JK, Kretschmer K, Freyer J, Floess S, Garbe A, Baron U, Olek S, Hamann A, von Boehmer H, Huehn J (2008) DNA methylation controls Foxp3 gene expression. Eur J Immunol 38:1654–1663
21. Nagar M, Vernitsky H, Cohen Y, Dominissini D, Berkun Y, Rechavi G, Amariglio N, Goldstein I (2008) Epigenetic inheritance of DNA methylation limits activation-induced expression of FOXP3 in conventional human CD25−CD4+ T cells. Int Immunol 20:1041–1055
22. Baron U, Floess S, Wieczorek G, Baumann K, Grutzkau A, Dong J, Thiel A, Boeld TJ, Hoffmann P, Edinger M, Turbachova I, Hamann A, Olek S, Huehn J (2007) DNA demethylation in the human FOXP3 locus discriminates regulatory T cells from activated FOXP3(+) conventional T cells. Eur J Immunol 37:2378–2389
23. Ma H, Liu G, Ding W, Wu Y, Cai L, Zhao Y (2008) Diabetes-induced alteration of F4/80+ macrophages: a study in mice with streptozotocin-induced diabetes for a long term. J Mol Med 86:391–400
24. Sun Z, Zhao L, Wang H, Sun L, Yi H, Zhao Y (2006) Presence of functional mouse regulatory CD4+CD25+T cells in xenogeneic neonatal porcine thymus-grafted athymic mice. Am J Transplant 6:2841–2850
25. Wang H, Zhao L, Sun Z, Sun L, Zhang B, Zhao Y (2006) A potential side effect of cyclosporin A: inhibition of CD4(+)CD25 (+) regulatory T cells in mice. Transplantation 82:1484–1492
26. Zheng QH, Ma LW, Zhu WG, Zhang ZY, Tong TJ (2006) p21Waf1/Cip1 plays a critical role in modulating senescence through changes of DNA methylation. J Cell Biochem 98:1230–1248
27. von Boehmer H, Teh HS, Kisielow P (1989) The thymus selects the useful, neglects the useless and destroys the harmful. Immunol Today 10:57–61
28. Sentman CL, Shutter JR, Hockenbery D, Kanagawa O, Korsmeyer SJ (1991) bcl-2 inhibits multiple forms of apoptosis but not negative selection in thymocytes. Cell 67:879–888
29. MacFarlane M, Jones NA, Dive C, Cohen GM (1996) DNA-damaging agents induce both p53-dependent and p53-independent apoptosis in immature thymocytes. Mol Pharmacol 50:900–911
30. Sakaguchi S (2005) Naturally arising Foxp3-expressing CD25 +CD4+ regulatory T cells in immunological tolerance to self and non-self. Nat Immunol 6:345–352
31. Shevach EM (2000) Regulatory T cells in autoimmmunity. Annu Rev Immunol 18:423–449
32. Kuniyasu Y, Takahashi T, Itoh M, Shimizu J, Toda G, Sakaguchi S (2000) Naturally anergic and suppressive CD25(+)CD4(+) T cells as a functionally and phenotypically distinct immunoregulatory T cell subpopulation. Int Immunol 12:1145–1155
33. Zhang A, Qu Y, Zhang B, Zhang L, Zeng C, Peng J, Ji X, Hou M, Zhao Y (2007) The different effects of indirubin on effector and CD4+CD25+ regulatory T cells in mice: potential implication for the treatment of autoimmune diseases. J Mol Med 85:1263–1270
34. Santini V, Kantarjian HM, Issa JP (2001) Changes in DNA methylation in neoplasia: pathophysiology and therapeutic implications. Ann Intern Med 134:573–586
35. Gorbunova V, Seluanov A, Mittelman D, Wilson JH (2004) Genome-wide demethylation destabilizes CTG.CAG trinucleotide repeats in mammalian cells. Hum Mol Genet 13:2979–2989
36. Baylin SB (2004) Reversal of gene silencing as a therapeutic target for cancer—roles for DNA methylation and its interdigitation with chromatin. Novartis Found Symp 259:226–233
37. Brunkow ME, Jeffery EW, Hjerrild KA, Paeper B, Clark LB, Yasayko SA, Wilkinson JE, Galas D, Ziegler SF, Ramsdell F (2001) Disruption of a new forkhead/winged-helix protein, scurfin, results in the fatal lymphoproliferative disorder of the scurfy mouse. Nat Genet 27:68–73
38. Lucifero D, Mertineit C, Clarke HJ, Bestor TH, Trasler JM (2002) Methylation dynamics of imprinted genes in mouse germ cells. Genomics 79:530–538
39. Nielsen J, Holm TL, Claesson MH (2004) CD4+CD25+ regulatory T cells: II. Origin, disease models and clinical aspects. Apmis 112:642–650
40. Kim JM, Rudensky A (2006) The role of the transcription factor Foxp3 in the development of regulatory T cells. Immunol Rev 212:86–98
41. Jordan MS, Boesteanu A, Reed AJ, Petrone AL, Holenbeck AE, Lerman MA, Naji A, Caton AJ (2001) Thymic selection of CD4 +CD25+ regulatory T cells induced by an agonist self-peptide. Nat Immunol 2:301–306
42. Walker LS, Chodos A, Eggena M, Dooms H, Abbas AK (2003) Antigen-dependent proliferation of CD4+ CD25+ regulatory T cells in vivo. J Exp Med 198:249–258
43. Caton AJ, Cozzo C, Larkin J 3rd, Lerman MA, Boesteanu A, Jordan MS (2004) CD4(+) CD25(+) regulatory T cell selection. Ann N Y Acad Sci 1029:101–114
44. Cihak A, Vesely J (1978) Effects of 5-aza-2′-deoxycytidine on DNA synthesis in mouse lymphatic tissues. Neoplasma 25:385–393
45. Cihak A, Vesely J (1979) Depression of DNA synthesis in mouse spleen after treatment with 5-aza-2′-deoxycytidine. J Natl Cancer Inst 63:1035–1039
46. Momparler RL, Frith CH (1981) Toxicology in mice of the antileukemic agent 5-aza-2′-deoxycytidine. Drug Chem Toxicol 4:373–381
47. Paessens LC, Fluitsma DM, van Kooyk Y (2008) Haematopoietic antigen-presenting cells in the human thymic cortex: evidence for a role in selection and removal of apoptotic thymocytes. J Pathol 214:96–103
48. Esashi E, Sekiguchi T, Ito H, Koyasu S, Miyajima A (2003) Cutting edge: a possible role for CD4+ thymic macrophages as professional scavengers of apoptotic thymocytes. J Immunol 171:2773–2777
49. Seitz HM, Camenisch TD, Lemke G, Earp HS, Matsushima GK (2007) Macrophages and dendritic cells use different Axl/Mertk/Tyro3 receptors in clearance of apoptotic cells. J Immunol 178:5635–5642
50. Devitt A, Parker KG, Ogden CA, Oldreive C, Clay MF, Melville LA, Bellamy CO, Lacy-Hulbert A, Gangloff S, Goyert SM, Gregory CD (2004) Persistence of apoptotic cells without autoimmune disease or inflammation in CD14−/− mice. J Cell Biol 167:1161–1170